

# †Explanation of the similarity of the photoemission spectra of SrVO<sub>3</sub> and CaVO<sub>3</sub>

I.A. Nekrasov,<sup>1,2</sup> G. Keller,<sup>2</sup> D.E. Kondakov,<sup>1,2,3</sup> A.V. Kozhevnikov,<sup>1,2,3</sup>  
Th. Pruschke,<sup>2</sup> K. Held,<sup>4</sup> D. Vollhardt,<sup>2</sup> and V.I. Anisimov<sup>1,2</sup>

<sup>1</sup>*Institute of Metal Physics, Russian Academy of Sciences-Ural Division, 620219 Yekaterinburg GSP-170, Russia*

<sup>2</sup>*Theoretical Physics III, Center for Electronic Correlations and Magnetism,  
University of Augsburg, 86135 Augsburg, Germany*

<sup>3</sup>*Department of Theoretical Physics and Applied Mathematics, USTU, 620002 Yekaterinburg Mira 19, Russia*

<sup>4</sup>*Max Planck Institute for Solid State Research, Heisenbergstr. 1, 70569 Stuttgart, Germany*

We present parameter-free LDA+DMFT results for the many-particle density of states of cubic SrVO<sub>3</sub> and orthorhombic CaVO<sub>3</sub>. Both systems are found to be strongly correlated metals, but *not* on the verge of a metal-insulator transition. In spite of the considerably smaller V-O-V bonding angle in CaVO<sub>3</sub> the photoemission spectra of the two systems are very similar, their quasiparticle parts being almost identical. This is in contrast to earlier theoretical and experimental conclusions, but in agreement with recent bulk-sensitive photoemission experiments.

PACS numbers: 71.27.+a, 71.30.+h

† **Joint theoretical and experimental paper on the same subject could be found on cond-mat/0312429.**

Transition metal oxides are an ideal laboratory for the study of electronic correlations in solids. Among these materials, cubic perovskites have the simplest crystal structure and thus may be viewed as a starting point for understanding the electronic properties of more complex systems. Typically, the  $3d$  states in those materials form comparatively narrow bands of width  $W \sim 2-3$  eV which lead to strong Coulomb correlations between the electrons. Particularly simple are transition metal oxides with a  $3d^1$  configuration since they do not show a complicated multiplet structure.

Intensive experimental investigations of spectral and transport properties of strongly correlated  $3d^1$  transition metal oxides started with the paper by Fujimori *et al.* [1]. These authors observed a pronounced lower Hubbard band in the photoemission spectra (PES) which cannot be explained by conventional band structure theory. A number of papers [2, 3] subsequently addressed the spectral, transport and thermodynamic properties of the  $3d^1$  series Sr<sub>1-x</sub>Ca<sub>x</sub>VO<sub>3</sub> for various values of  $x$ , yielding contradictory results. While the thermodynamic properties (Sommerfeld coefficient, resistivity, and paramagnetic susceptibility) were found to be essentially independent of  $x$  from  $x=0$  (SrVO<sub>3</sub>) to  $x=1$  (CaVO<sub>3</sub>) [2], PES and Bremsstrahlungs isochromat spectra (BIS) [3] showed drastic differences. In fact, the spectroscopic data seemed to imply that this substitution series develops from a strongly correlated metal (SrVO<sub>3</sub>) into, practically, an insulator (CaVO<sub>3</sub>), i.e., that for  $x \rightarrow 1$  Sr<sub>1-x</sub>Ca<sub>x</sub>VO<sub>3</sub> is on the verge of a Mott-Hubbard transition.

An experimental answer to this puzzle was very recently provided by bulk-sensitive PES obtained by Maiti *et al.* [4], and especially by high-resolution bulk-sensitive PES measured by Sekiyama *et al.* [5]. In the latter work it was shown that (i) the technique of prepar-

ing the sample surface (which should preferably be done by fracturing) is very important, and that (ii) the energy of the X-ray beam should be large enough to increase the photoelectron escape depth to achieve bulk-sensitivity; also the beam should provide a high instrumental resolution (about 100 meV in [5]). With these experimental improvements the PES of SrVO<sub>3</sub> and CaVO<sub>3</sub> were found to be almost identical [4, 5], implying consistency of spectroscopic and thermodynamic results at last. This is also in accord with earlier 1s x-ray absorption spectra (XAS) by Inoue *et al.* [6] which differ only slightly above the Fermi energy, in contrast to the BIS data [3].

The main effect of substituting Sr ions by the isovalent, but smaller, Ca ions is to decrease the V-O-V angle from  $\theta = 180^\circ$  in SrVO<sub>3</sub> [7] to  $\theta \approx 162^\circ$  [8] in the orthorhombically distorted  $Pbnm$  structure of CaVO<sub>3</sub> [9]. This bond bending results in a decrease of the one-particle bandwidth  $W$  and thus in an increase of the ratio  $U/W$  as one moves from SrVO<sub>3</sub> to CaVO<sub>3</sub>. Within a one-band Hubbard model, neglecting the orbital structure of the V  $3d$ , Rozenberg *et al.* [10] were able to fit the more surface-sensitive spectroscopic data for Sr<sub>1-x</sub>Ca<sub>x</sub>VO<sub>3</sub> and, with other parameters, the bulk-sensitive PES [4].

In this Letter we present results of a parameter-free, comparative study of SrVO<sub>3</sub> and CaVO<sub>3</sub> using the recently developed LDA+DMFT computational scheme [11, 12, 13, 14, 15, 16], which merges the local density approximation (LDA) with a modern many-body technique, the dynamical mean-field theory (DMFT) [17]. In this realistic approach the orbital degrees of freedom of the three partially filled  $t_{2g}$  bands are explicitly taken into account [1], resulting in a spectral weight distribution distinctly different from that of a one-band model.

We first discuss the electronic and crystal structure of SrVO<sub>3</sub> and CaVO<sub>3</sub>. The valence states of these two systems consist of completely occupied oxygen  $2p$  bands and partially occupied V- $3d$  bands. There is one electron oc-

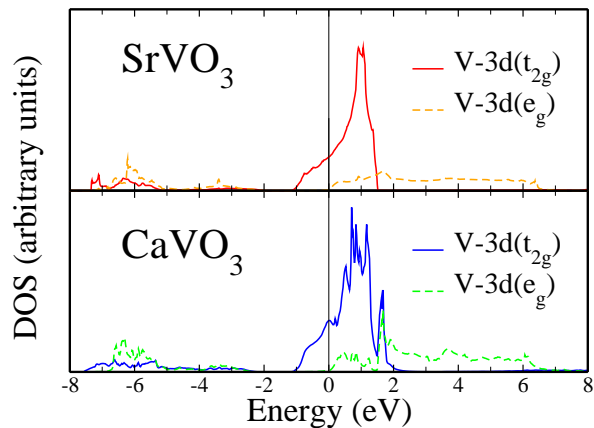


FIG. 1: Partial DOS of the V-3d  $t_{2g}$  band (solid line) and  $e_g$  band (dashed line) for SrVO<sub>3</sub> and CaVO<sub>3</sub> calculated by the LDA-LMTO method. The Fermi level corresponds to zero energy.

cupying the  $d$ -states per V ion ( $d^1$  configuration). Fig. 1 shows the LDA density of states (DOS) for both compounds which we obtained via the TBLMTO47 code of Andersen and coworkers [18, 19], using the crystal structure data of Refs. [7, 8].

In both compounds the V ions are in an octahedral oxygen coordination. The octahedral crystal field splits the V-3d states into three degenerate  $t_{2g}$  and two degenerate  $e_g$  states. While a hybridization between these  $t_{2g}$  and  $e_g$  states is forbidden for the cubic SrVO<sub>3</sub> crystal, the distorted orthorhombic structure of CaVO<sub>3</sub> allows them to mix. In Fig. 1 one can see some contributions of the  $t_{2g}$  and  $e_g$  subbands in the energy range from -8 eV to -2 eV due to the hybridization with O-2p states. They amount to 12% and 15% of all  $t_{2g}$  states in SrVO<sub>3</sub> and CaVO<sub>3</sub>, respectively. The  $t_{2g}$  states are dominant in the vicinity of the Fermi energy, the center of gravity of the  $e_g$  band lying above the upper band edge of the  $t_{2g}$  band. Therefore the low energy physics (<1.5 eV) is governed by the  $t_{2g}$  bands which can be considered sufficiently separated from the  $e_g$  states in both compounds.

We concentrate on this energy range in Fig. 2, where we compare the LDA  $t_{2g}$  DOS of SrVO<sub>3</sub> and CaVO<sub>3</sub>. Most importantly, the one-electron  $t_{2g}$  bandwidth of CaVO<sub>3</sub>, defined as the energy interval where the DOS in Fig. 2 is non-zero, is found to be only 4% smaller than that of SrVO<sub>3</sub> ( $W_{\text{CaVO}_3} = 2.5$  eV,  $W_{\text{SrVO}_3} = 2.6$  eV). One would have expected that the strong lattice distortion with a decrease of the V-O-V bond angle from 180° to 162° affects the  $t_{2g}$  bandwidth much more strongly. Such a larger effect indeed occurs in the  $e_g$  bands whose bandwidth is reduced by 10%. To physically understand the smallness of the narrowing of the  $t_{2g}$  bands we have calculated the effective  $t_{2g}$ - $t_{2g}$  and  $e_g$ - $e_g$  hopping parameters. The predominant contribution to the  $e_g$ - $e_g$  hopping is through a  $d$ - $p$ - $d$  hybridization, which is considerably decreasing with the lattice distortion. This is also the

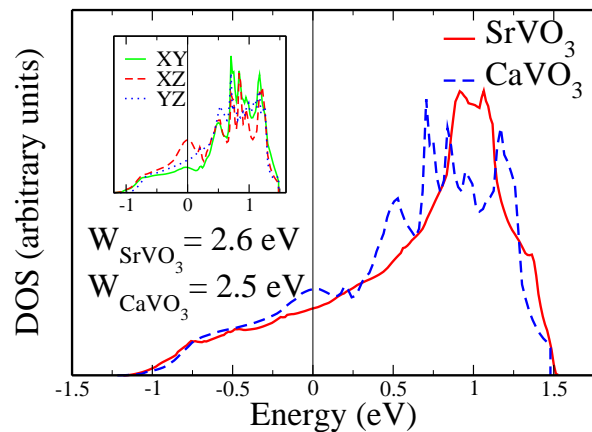


FIG. 2: Comparison of the LDA DOS of the V-3d  $t_{2g}$  band for SrVO<sub>3</sub> (solid line) and CaVO<sub>3</sub> (dashed line). In CaVO<sub>3</sub> the degeneracy of the three  $t_{2g}$  bands is lifted (see inset). The bandwidth  $W_{\text{CaVO}_3} = 2.5$  eV is only 4% smaller than  $W_{\text{SrVO}_3} = 2.6$  eV.

case for the  $t_{2g}$  orbitals. However, for the  $t_{2g}$  orbitals the direct  $d$ - $d$  hybridization is also important. This hybridization *increases* with the distortion since the  $t_{2g}$  orbital lobes point more directly towards each other in the distorted structure. Altogether, the competition between i) decreasing  $d$ - $p$ - $d$  hybridization and ii) increasing  $d$ - $d$  hybridization results in a very small change of the  $t_{2g}$  bandwidth. This explains why previous suggestions of strongly different bandwidths are untenable.

As is well-known, LDA does not treat the effects of strong local Coulomb correlations adequately. To overcome this drawback, we use LDA+DMFT as a non-perturbative approach to study strongly correlated systems [11, 16]. It combines the strength of the LDA in describing weakly correlated electrons in the  $s$ - and  $p$ -orbitals, with the DMFT treatment of the dynamics due to local Coulomb interactions. In the present paper we will discuss the relevant parts of the LDA+DMFT approach only briefly, referring the reader to Ref. [16] for details.

Given a specific material, it is possible to extract from the LDA band structure a one-particle Hamiltonian  $\hat{H}_{\text{LDA}}^0$  where the averaged Coulomb interaction is subtracted to avoid double counting [11]. Supplementing  $\hat{H}_{\text{LDA}}^0$  with the local Coulomb interactions between the electrons one arrives at a material-specific Hamiltonian which includes correlations:

$$\hat{H} = \hat{H}_{\text{LDA}}^0 + U \sum_m \sum_i \hat{n}_{im\uparrow} \hat{n}_{im\downarrow} + \sum_i \sum_{m \neq m'} \sum_{\sigma \sigma'} (U' - \delta_{\sigma \sigma'} J) \hat{n}_{im\sigma} \hat{n}_{im'\sigma'}. \quad (1)$$

In the present case, the index  $i$  enumerates the V sites,  $m$  denotes the individual  $t_{2g}$  orbitals, and  $\sigma$  is the spin. Because of the nearly cubic symmetry of CaVO<sub>3</sub>, one can simplify the calculation and use only the one-particle

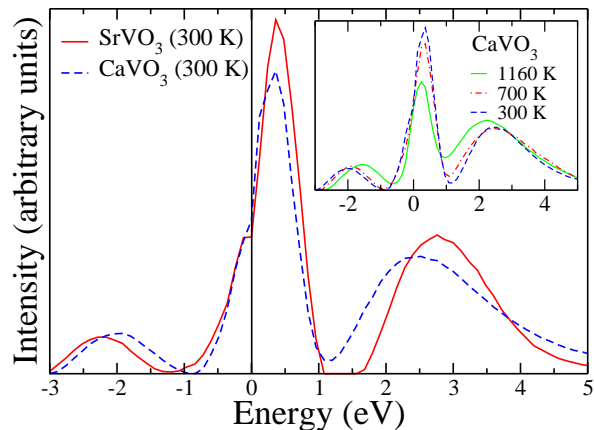


FIG. 3: LDA+DMFT(QMC) spectrum of SrVO<sub>3</sub> (solid line) and CaVO<sub>3</sub> (dashed line) calculated at T=300 K (inset: effect of temperature in the case of CaVO<sub>3</sub>).

LDA DOS  $N^0(\epsilon)$  of Fig. 2 instead of the full Hamiltonian  $\hat{H}_{\text{LDA}}^0$  [16]. In Eq. (1), the local intra-orbital Coulomb repulsion  $U$ , the inter-orbital repulsion  $U'$ , and the exchange interaction  $J$  are explicitly taken into account. We calculated these interaction strengths by means of the constrained LDA method [20] for SrVO<sub>3</sub>, allowing the  $e_g$  states to participate in screening [21]. The resulting value of the averaged Coulomb interaction is  $\bar{U} = 3.55$  eV ( $\bar{U} = U'$  for  $t_{2g}$  orbitals [16, 22]) and  $J = 1.0$  eV. The intra-orbital Coulomb repulsion  $U$  is then fixed by rotational invariance to  $U = U' + 2J = 5.55$  eV. We did not calculate  $\bar{U}$  for CaVO<sub>3</sub> because the standard procedure to calculate the Coulomb interaction parameter between two  $t_{2g}$  electrons which are screened by  $e_g$  states is not applicable for the distorted crystal structure where the  $e_g$  and  $t_{2g}$  orbitals are not separated by symmetry. On the other hand, it is well-known that the change of the *local* Coulomb interaction is typically much smaller than the change in the DOS, which was found to depend only very weakly on the bond angle. That means that  $\bar{U}$  for CaVO<sub>3</sub> should be nearly the same as for SrVO<sub>3</sub>. Therefore we used  $\bar{U} = 3.55$  eV and  $J = 1.0$  eV for both SrVO<sub>3</sub> and CaVO<sub>3</sub>. This is also in agreement with previous calculations of vanadium systems [21] and experiments [26].

The Hamiltonian (1) is solved within the DMFT using standard quantum Monte-Carlo (QMC) techniques to solve the self-consistency equations [27]. From the imaginary time QMC Green function we calculate the physical (real frequency) spectral function with the maximum entropy method. The resulting LDA+DMFT(QMC) spectra for SrVO<sub>3</sub> and CaVO<sub>3</sub> in Fig. 3 show genuine correlation effects, i.e., the formation of lower Hubbard bands at about  $-1.5$  eV and upper Hubbard bands at about  $2.5$  eV, with well pronounced quasiparticle peaks at the Fermi energy. Therefore both SrVO<sub>3</sub> and CaVO<sub>3</sub> are strongly correlated metals. The 4% difference in the LDA bandwidth between SrVO<sub>3</sub> and CaVO<sub>3</sub> is only reflected in some additional transfer of spectral weight from the

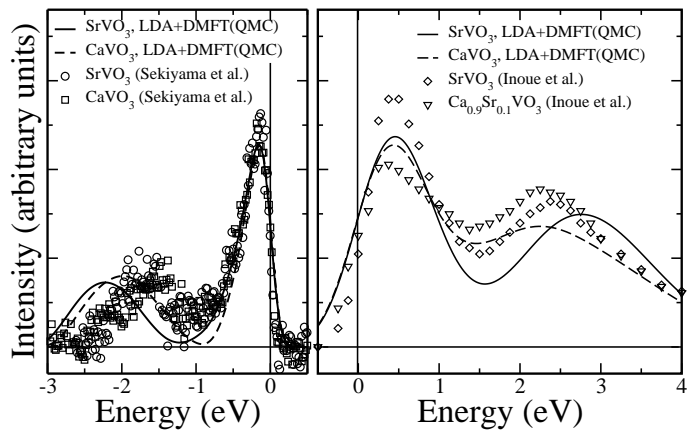


FIG. 4: Comparison of the calculated, parameter-free LDA+DMFT(QMC) spectra of SrVO<sub>3</sub> (solid line) and CaVO<sub>3</sub> (dashed line) with bulk-sensitive high-resolution PES (SrVO<sub>3</sub>: circles; CaVO<sub>3</sub>: rectangles) [5] (left panel) and 1s XAS spectra (SrVO<sub>3</sub>: diamonds; Ca<sub>0.9</sub>Sr<sub>0.1</sub>VO<sub>3</sub>: triangles) [6] (right panel). Horizontal line: experimental subtraction of the background intensity.

quasiparticle peak to the Hubbard bands, and minor differences in the positions of the Hubbard bands. Clearly, the two systems are not on the verge of a Mott-Hubbard metal-insulator transition. The many-particle DOS of the two systems shown in Fig. 3 are seen to be quite similar but not identical. In fact, SrVO<sub>3</sub> is slightly less correlated than CaVO<sub>3</sub>, in accord with their different LDA bandwidth. The inset of Fig. 3 shows that the effect of temperature on the spectrum is small for  $T \lesssim 700$  K. Due to the high photon energy the PES transition matrix elements will not significantly affect the distribution of spectral weight in the energy range considered here.

In the left panel of Fig. 4 we compare our LDA+DMFT spectra (300K), which were multiplied with the Fermi function at the experimental temperature (20 K) and Gauss broadened with the experimental resolution of  $0.1$  eV [5], to the experimental PES data obtained by subtracting estimated surface and oxygen contributions. The quasiparticle peaks in theory and experiment are seen to be in very good agreement. In particular, their height and width are almost identical for both SrVO<sub>3</sub> and CaVO<sub>3</sub>. The difference in the positions of the lower Hubbard bands may be partly due to (i) the subtraction of the (estimated) oxygen contribution which might also remove some  $3d$  spectral weight below  $-2$  eV, and (ii) uncertainties in the *ab-initio* calculation of  $\bar{U}$ . In the right panel of Fig. 4 we compare to the XAS data [6]. We consider core-hole life time effects by Lorentz broadening the spectrum with  $0.2$  eV [23], multiplying with the inverse Fermi function (80K), and then Gauss broadening with the experimental resolution of  $0.36$  eV [24]. Again, the overall agreement of the weights and positions of the quasiparticle and upper  $t_{2g}$  Hubbard band is good, including the tendencies when going from SrVO<sub>3</sub> to

CaVO<sub>3</sub> (Ca<sub>0.9</sub>Sr<sub>0.1</sub>VO<sub>3</sub> in the experiment). For CaVO<sub>3</sub> the weight of the quasiparticle peak is somewhat lower than in the experiment. In contrast to the one-band Hubbard model calculation, our material specific results reproduce the strong asymmetry around the Fermi energy w.r.t. weights and bandwidths. Our results also give a different interpretation of the XAS than in [6] where the maximum at about 2.5 eV was attributed to a  $e_g$  band and not to the  $t_{2g}$  upper Hubbard band [25]. The slight differences in the quasiparticle peaks (see Fig. 3) lead to different effective masses, namely  $m^*/m_0 = 2.1$  for SrVO<sub>3</sub> and  $m^*/m_0 = 2.4$  for CaVO<sub>3</sub>. These theoretical values agree with  $m^*/m_0 = 2 - 3$  for SrVO<sub>3</sub> and CaVO<sub>3</sub> as obtained from de Haas-van Alphen experiments and thermodynamics [2, 28]. We note that the effective mass of CaVO<sub>3</sub> obtained from optical experiments is somewhat larger, i.e.,  $m^*/m_0 = 3.9$  [26].

In summary, we investigated the spectral properties of the correlated  $3d^1$  systems SrVO<sub>3</sub> and CaVO<sub>3</sub> within the LDA+DMFT(QMC) approach. Constrained LDA was used to determine the average Coulomb interaction as  $\bar{U} = 3.55$  eV and the exchange coupling as  $J = 1.0$  eV. With this input we calculated the spectra of the two systems in a parameter-free way. Both systems are found to be strongly correlated metals, with a transfer of most of the spectral weight from the quasiparticle peak to the incoherent upper and lower Hubbard bands. Although the calculated DMFT spectra of SrVO<sub>3</sub> and CaVO<sub>3</sub> are slightly different above the Fermi energy the spectra below the Fermi energy are the resulting PES are very similar, the quasiparticle parts being almost identical. Our calculated spectra agree very well with recent bulk-sensitive high-resolution PES [5] and XAS [6], i.e., with the experimental spectrum below and above the Fermi energy. Both compounds are similarly strongly correlated metals; CaVO<sub>3</sub> is not on the verge of a Mott-Hubbard transition.

Our results are in striking contrast to previous theories and the widespread expectation that the strong lattice distortion leads to a strong narrowing of the CaVO<sub>3</sub> bandwidth and, hence, much stronger correlation effects in CaVO<sub>3</sub>. While the  $e_g$  bands indeed narrow considerably, the competition between decreasing  $d-p-d$  and increasing  $d-d$  hybridization leads to a rather insignificant narrowing of the  $t_{2g}$  bands at the Fermi energy. This explains why CaVO<sub>3</sub> and SrVO<sub>3</sub> are so similar. With our theoretical results confirming the new PES and XAS experiments, we conclude that the insulating-like behavior observed in earlier PES and BIS experiments on CaVO<sub>3</sub> must be attributed to surface effects [29].

This research was supported in part by the Deutsche Forschungsgemeinschaft through SFB 484 and the Emmy-Noether program, the Russian Foundation for Basic Research through RFFI-01-02-17063 and RFFI-03-02-06126, the Ural Branch of the Russian Academy of Sciences for Young Scientists, Grant of the President of Rus-

sia MK-95.2003.02, and the National Science Foundation under Grant No. PHY99-07949. We thank A. Sandvik for making available his maximum entropy code and acknowledge valuable discussions with I. H. Inoue, S. Suga, A. Fujimori, R. Claessen, and M. Mayr.

- [1] A. Fujimori *et al.*, Phys. Rev. Lett. **69**, 1796 (1992).
- [2] Y. Aiura *et al.*, Phys. Rev. B **47**, 6732 (1993); I. H. Inoue *et al.*, Phys. Rev. Lett. **74**, 2539 (1995); I. H. Inoue *et al.*, Phys. Rev. B **58**, 4372 (1998).
- [3] K. Morikawa *et al.*, Phys. Rev. B **52**, 13711 (1995).
- [4] K. Maiti *et al.*, Europhys. Lett. **55**, 246 (2001).
- [5] A. Sekiyama *et al.*, cond-mat/0206471.
- [6] I. H. Inoue *et al.*, Physica C **235-240**, 1007 (1994).
- [7] M.J. Rey *et al.*, J. Solid State Chem. **86**, 101 (1990).
- [8] M.H. Jung, and H. Nakotte, unpublished.
- [9] B. L. Chamberland and P. S. Danielson, J. Solid State Chem. **3**, 243 (1971).
- [10] M. J. Rozenberg *et al.*, Phys. Rev. Lett. **76**, 4781 (1996).
- [11] V. I. Anisimov *et al.*, J. Phys. Cond. Matter **9**, 7359 (1997); A. I. Lichtenstein and M. I. Katsnelson, Phys. Rev. B **57**, 6884 (1998).
- [12] A. Liebsch and A. Lichtenstein, Phys. Rev. Lett. **84**, 1591 (2000).
- [13] I. A. Nekrasov *et al.*, Euro. Phys. J. B **18**, 55 (2000); K. Held *et al.*, Phys. Rev. Lett. **86**, 5345 (2001); I. A. Nekrasov *et al.*, Phys. Rev. B **67**, 085111 (2003).
- [14] A. I. Lichtenstein, M. I. Katsnelson, and G. Kotliar, Phys. Rev. Lett. **87**, 67205 (2001). S. Biermann *et al.*, cond-mat/0112430.
- [15] S. Y. Savrasov, G. Kotliar, and E. Abrahams, Nature **410**, 793 (2001).
- [16] K. Held *et al.*, Psi-k Newsletter 56, 65 (2003) [psi-k.dl.ac.uk/newsletters/News\_56/Highlight\_56.pdf].
- [17] W. Metzner and D. Vollhardt, Phys. Rev. Lett. **62**, 324 (1989); A. Georges *et al.*, Rev. Mod. Phys. **68**, 13 (1996).
- [18] O. K. Andersen, Phys. Rev. B **12**, 3060 (1975); O. Gunnarsson, O. Jepsen, and O. K. Andersen, Phys. Rev. B **27**, 7144 (1983).
- [19] Our results are in agreement with LDA calculations in the basis of augmented plane waves (APW) by Takegahara (K. Takegahara, J. Electron Spectrosc. Relat. Phenom. **66**, 303 (1995)). For our purposes, i.e., for the combination of the LDA band structure with DMFT [11], the atomic-like wave functions basis set of the LMTO method is more appropriate.
- [20] O. Gunnarsson *et al.*, Phys. Rev. B **39**, 1708 (1989).
- [21] I. Solovyev, N. Hamada, and K. Terakura, Phys. Rev. B **53**, 7158 (1996).
- [22] M. B. Zöfl *et al.*, Phys. Rev. B **61**, 12810 (2000).
- [23] M. O. Krause and J. H. Oliver, J. Phys. Chem Ref. Data **8**, 329 (1979).
- [24] I. H. Inoue, private communication.
- [25] From the centers of gravity of the LDA DOS (Fig. 1), we would expect the correlated  $e_g$  states to form an upper Hubbard band with center of gravity at roughly 2.5 eV above the upper Hubbard band of the  $t_{2g}$  states, with the  $e_g$  Hubbard band being very flat.
- [26] H. Makino *et al.*, Phys. Rev. B **58**, 4384 (1998);
- [27] J. E. Hirsch and R. M. Fye, Phys. Rev. Lett. **56**, 2521 (1986). For multi-band QMC within DMFT see [16].
- [28] I. H. Inoue *et al.*, Phys. Rev. Lett. **88**, 236403 (2002).
- [29] During the completion of this paper DMFT results for surface and bulk spectra of SrVO<sub>3</sub> were reported by A.

Liebsch Phys. Rev. Lett. **90**, 096401 (2003).